Beam Diagnostics Instrumentation for a 6.7-MeV Proton Beam Halo Experiment•

J. D. Gilpatrick, D. Barr, D. Bruhn, L. Day, K. U. Kasemir, J. Ledford, M. Pieck, W. Sellyey, R. Shurter, M. Stettler, R. Valdiviez, LANL, Los Alamos, NM, 87545, USA;
J. Kamperschroer, D. Martinez, General Atomics, San Diego, CA, 92186, USA;
J. O'Hara, M. Gruchalla, Honeywell, Los Alamos, NM, 87544, USA;
D. Madsen, ARES Corporation, Los Alamos, NM, 87544, USA

Abstract

A 52 quadrupole-magnet FODO lattice is presently being installed in the Low Energy Demonstration Accelerator (LEDA) facility between the radio frequency quadrupole (RFQ) and a high-energy beam transport (HEBT) [1]. The purpose of this lattice is to provide a beam transport to measure the formation of beam halo and compare the measured data with halo simulations. To attain this goal, several types of beam-diagnostic instruments are being installed in the magnet lattice. There will be nine beam-profile-measurement stations. Each station will have use of a slow wire scanner to detect the projected-distribution beam core, and a set of graphite or copper scrapers that measures the "tails" of the distribution down to 0.01% of the distribution peak. Also included in the instrumentation suite are ten beam position monitors (BPM), five beam loss monitors (BLM), three pulsed-current toroids, and an energy measurement similar to existing beam instrumentation [2,3]. This paper describes the instruments, initial test data, and their expected performance.

1 HALO EXPERIMENT LAYOUT

The primary purpose of a 52-quadrupole-magnet FODO lattice is to provide a vehicle to measure phase-space halo. The quadrupole magnets are spaced every 21 cm so that beam measurement hardware may be interspersed between the magnets. Pictured in Fig. 1 are most of the beam measurement hardware consisting of a wire scanner and halo-scraper assembly (WS/HS), beam-position monitors, a pulsed-beam-current transformer, a resistive-wall-current monitor (RWCM) for monitoring the central beam phase and energy, and loss monitors (not pictured).

The first four quadrupole magnets in the lattice are independently powered so that their gradients can be adjusted to match and mismatch the RFQ output beam to the lattice. Depending on how the magnets are adjusted, the development of specific types of halo is possible. These phase space halos manifest themselves as various shapes or "shoulders" on the projected beam distributions as measured by the WS/HS assemblies [4].

Table 1 shows the locations of various beam diagnostic components and steering dipole magnets as defined by the space upstream of the numbered quadrupole magnet. The WS/HS assemblies measure projected beam distributions in both horizontal and vertical planes at 9 locations within the lattice. The first WS/HS located at quadrupole magnet #5 is used to verify the RFQ-output-beam distribution. The two sets of four WS/HS provide beam matching and rms beam emittance information in the middle and end of the transport lattice. The set of four WS/HS assemblies located between magnets 21 and 27 measure the beam's match condition after the beam has sufficiently debunched to reduce any longitudinal space charge issues. The set of four WS/HS assemblies located between magnets 46 and 52 provide sufficient mismatch information to detect two possible mismatch modes, the quadrupole and "breathing" modes [4].

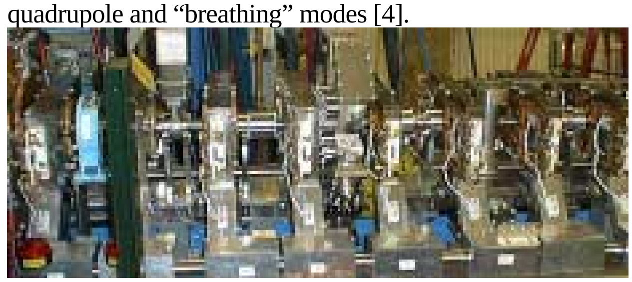

Figure 1. Shown above are the initial 8 quadrupole magnets , 2 steering magnets, and the initial beam diagnostic instruments in the quadrupole-magnet lattice.

Table 1. Halo lattice beamline component locations

Device	Locations (Quadrupole Magnet #)
WS/HS	5, 21, 23, 25, 27, 46, 48, 50, 52
BPM	6, 8, 17, 19, 28, 30, 38, 40, 49, 51
Steerers	4, 6, 15, 17, 26, 28, 36, 38, 47, 49
BLM	5, 16, 27, 37, 48
Toroid	2, 24, 44
RWCM	4, 9

The beam-steering plan corrects the beams position at the end of every set of BPM/associated steering magnet pairs separated by approximately 10 quadrupole magnets (see Table 1). Since the FODO-lattice period has a phase advance of approximately 80 degrees, each pair of BPMs can detect and each pair of steering magnets can correct the beam position and angle.

• This work supported by the Department of Energy.

Pulsed current measurements are monitored at the beginning, middle, and end of the transport lattice. Loss measurements are located over the steering-magnets approximately 1 m from the beam line center. Finally, there is a set of RWCMs to allow for the measurement of the time of flight of the bunched beam so that central beam energy and phase may be measured.

2 BEAM PROFILES: WS/HS

The WS/HS mechanical beamline device, pictured in fig. 2, has two types of measurement devices that provide projected beam distribution information: a slow wire scanner and a pair of water-cooled graphite scrapers [5]. For each axis, there is a movable slow wire scanner that measures the beam core distribution, i.e., inside +/- 3 rms widths. Secondary electrons emitted from the 0.033-mm C monofilament provide a relative beam charge density versus transverse wire location. The beam–distribution edges outside 2.5 rms widths, are measured by graphite scrapers. Since the 6.7-MeV protons range out in C in < 0.3 mm, the 1.5-mm thick graphite scrapers capture all of the beam. It is necessary to cool the graphite so a water-cooled Cu plate is brazed to the back of the graphite scraper [6]. These graphite scrapers are biased so that the proton-beam charge is collected and secondary electron emission is inhibited.

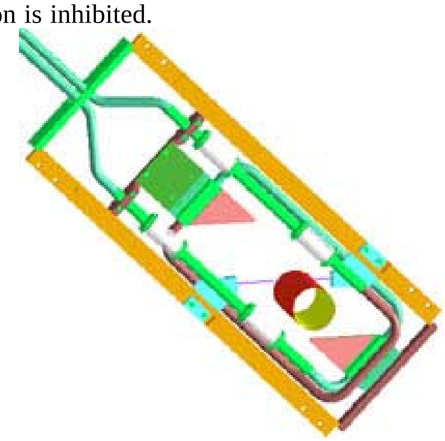

Figure 2. The horizontal WS/HS assembly pictured above contains both a wire scanner and two halo scrapers. A similar assembly oriented normal to this assembly provides vertical beam profile information.

Fig. 3 shows the result of what is expected from the combination of the wire scanner and scraper signals given a 1-mm-rms-width gaussian-distributed beam (i.e., expected match condition of the beam exiting the RFQ). There were four types of noise modeled: time-dependent beam current and position variations, wire placement error, and thermal signal-to-noise errors. The scraper data are normalized to the wire scanner data between 2.5 and 3 rms widths. Note that under these conditions we should be capable of measuring beam to approximately 5 rms widths.

The WS/HS detection electronics for two beamline locations are contained in a single-wide VXI module. The detection is accomplished by using a lossy integrator circuit to integrate the charge interacting with either the scanner or scraper. The resistor and capacitor in the amplifier feedback path were selected to optimize the amplifier's signal to noise and to be adequately discharged within 0.1 s. The signals are then digitized and passed to the EPICS control system [7].

Wire and scraper movement is accomplished by rotating the attached lead-screw assembly with a Compumotor OS22B-series stepper motor. The motor is controlled with a National Instruments PXI-7344 controller and the associated driver. The wire and scraper position is reported to the controller with a Dynamics Research Corporation linear optical encoder.

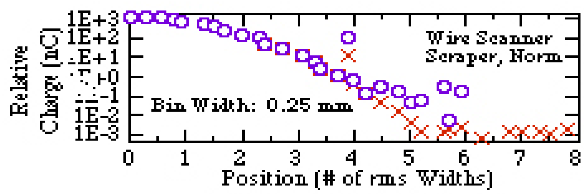

Figure 3. Simulation of beam distribution with four types of noise imposed on the signal.

The EPICS control system uses portable channel access to pass process variables, such as a new wire location, to a National Instruments LabVIEW® virtual instrument (VI) running on a local computer. The VI then instructs the motor controller to move the motor and reports the new position once the controller has detected from the encoder that it has arrived.

3 PULSED BEAM CURRENT

The pulsed-beam current measurement hardware is a high–permeability 122-mm-ID X 156-mm-OD X 30-mm-long core with two sets of windings: a secondary and calibration winding (see Fig. 4). The secondary winding provides a +/- 4 V signal to an ADC for a 100-mA beam current. Fig. 4 also shows the steel cover that provides additional external-magnetic-field shielding. The secondary winding signal is then fed to an ADC within a single-wide beam-current VXI module [8]. This module has within it a pulsed current source that provides a calibrated method to verify the overall measurement accuracy. The toroids have been measured to have < 6%/ms droop and a < 1µs rise time which is equivalent to an approximate 0.009- to 620-kHz bandwidth.

4 BEAM LOSS

For previous LEDA beam measurements, ionization chambers (IC) were used to measure the ionizing radiation resulting from beam impinging on beam-line structures [9]. However, the amount of radiation and IC signal was 0.1 of what was initially expected resulting in a noisy measurement. To improve the loss monitor sensitivity, photomultiplier tubes (PMT) with a CsI scintillator have been ordered from Bicron. The output signal of these devices one meter from the beam line will be 1 μA per lost mA of beam current. The 170-kHz bandwidth of the associated electronics will allow for observation of structure in beam loss during 20-μs-long beam-pulses.

Figure 4. Bergoz ACCTs are installed with additional external magnetic-field shielding.

5 BEAM POSITION

The BPMs are a standard 4-electrode micro-stripline design with an electrode aperture of 2.9 cm and a subtended angle of 45 degrees (see fig. 5). The mapped wire-based sensitivity was measured to be 2.170 +/- 0.005 dB/mm and with offsets no greater than +/- 0.5 dB.

Figure 5. All of the BPMs have a sensitivity of 2.170 +/- 0.005 dB/mm and offsets < +/-0.5 dB.

The BPM electrode signals are fed to a VXI module that contains four independent AD8307 successive-approximation amplifier channels. Each electrode's signal is detected, amplified, and digitized so that the signals from opposite electrodes may be subtracted, thereby creating a log-ratio processor [10]. Fig. 6 shows a typical result of this subtraction. Within the processor, the calibrator can inject signals either through the BPM or through the processor to correct the errors shown in fig. 6 to < +/-0.05 dB [11].

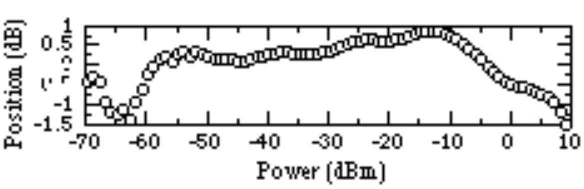

Figure 6. Position electronics uncorrected-error over the operational dynamic range of the circuitry.

5 BEAM ENERGY AND PHASE

The central beam energy is measured using two RWCMs. Their design was optimized for detecting the phase of the 350-MHz bunched beam. Thirty-six 1.8-kΩ resistors are soldered across a short ceramic vacuum break. A small ferromagnetic core provides sufficient inductance to produce a low corner frequency of approximately 100 MHz. With a drift distance of approximately 1.05 m, 1-keV resolution time-of-flight energy measurements will be made [12].

REFERENCES

[1] P. L. Colestock, et al., "The Beam Halo Experiment at the LEDA Facility: a First Test of the Core-Halo Model," this conference.

[2] J. D. Gilpatrick, et al., "Beam Diagnostic Instrumentation for the Low–Energy Demonstration Accelerator (LEDA): Commissioning and Operational Experience", EPAC'00, Vienna, Austria, June 25-30, 2000.

[2] J. D. Gilpatrick, et al., "LEDA Beam Diagnostics Instrumentation: Measurement Comparisons and Operational Experience", BIW '00, Boston, MA, May 8-11, 2000.

[3] T. Wangler, et al., "Beam Halo in Proton Linac Beams," this conference.

[5] R. Valdiviez, et al., "Intense Proton Core And Halo Beam Profile Measurement: Beam Line Component Mechanical Design," this conference.

[6] J. O'Hara, et al., "Slow Wire Scanner Beam Profile Measurement for LEDA", BIW '00, Boston, MA, May 8-11, 2000.

[7] L. Day, et al., "Control System for the LEDA 6.7-MeV Proton Beam Halo Experiment", this conference.

[8] D. Barr, et al., "LEDA Beam Diagnostics Instrumentation: Beam Current Measurement", BIW '00, Boston, MA, May 8-11, 2000.

[9] W. Sellyey, et al., "Experience With Beam Loss Monitors In The Low Energy Demonstration Accelerator (LEDA)", BIW '00, Boston, MA, May 8-11, 2000.

[10] D. Barr, et al., "LEDA Beam Diagnostics Instrumentation: Beam Position Monitors," BIW '00, Boston, MA, May 8-11, 2000.

[11] R. B. Shurter, et al., "BPM Analog Front End Electronics Based on the AD8307 Log Amplifier", BIW '00, Boston, MA, May 8-11, 2000.

[12] J. F. Power, et al., "Performance of the Beam Phase Measurement System for LEDA", BIW '00, Boston, MA, May 8-11, 2000.